arXiv:1206.6797v1 [cond-mat.str-el] 28 Jun 2012

Correlated Phases of Population Imbalanced Fermi-Fermi Mixtures on an Optical Lattice

Chen-Yen Lai, Chuntai Shi, and S.-W. Tsai*
Department of Physics and Astronomy, University of California, Riverside, California 92521, USA

(Dated: June 29, 2012)

We study a two species fermion mixture with different populations on a square lattice modeled by a Hubbard Hamiltonian with on-site inter-species repulsive interaction. Such a model can be realized in a cold atom system with fermionic atoms in two different hyperfine states loaded on an optical lattice and with tunable inter-species interaction strength via external fields. For a two-dimensional square lattice, when at least one of the fermion species is close to half-filling, the system is highly affected by lattice effects. With the majority species near half-filling and varying densities for the minority species, we find that several correlated phases emerge as the ground state, including a spin density wave state, a charge density wave state with stripe structure, and various p-wave BCS pairing states for both species. We study this system using a functional renormalization group method, determine its phase diagram at weak coupling, discuss the origin and characteristics of each phase, and provide estimates for the critical temperatures.

PACS numbers: 71.10.Fd 67.85.Lm 05.30.Fk 05.10.Cc 71.10.Hf

Introduction - Experiments with ultra-cold atoms have realized mixtures of two different species of fermionic atoms with different densities, including mixtures of cold lithium atoms (^{6}Li) with different populations for two different hyperfine states[1–6]. Fermionic systems with imbalanced spin populations have been studied in electronic materials, such as magnetic-field-induced organic superconductors[7, 8]. Mixtures of different species of fermions with unequal populations have also been considered in the study of quark matter[9]. With the rapid experimental advances in the field of cold atom physics, these systems have the advantage of a great degree of tunability and control of inter-particle interactions, dimensionality, confinement, as well as number of pseudo-spin species. Imbalanced mixtures of cold fermionic atoms have attracted great interest due to their possible rich phase diagram[6]. Several phases have been observed experimentally[5, 6], such as imbalanced superfluid phase, phase separation, and normal Fermi liquid behavior. Also, Larkin-Ovchinnikov-Fulde-Ferrel (LOFF) state[10], which involves Cooper pairs with finite center-of-mass momentum, and breached pair[11, 12] state with zero center-of-mass momentum, could be possible phases in special regions of the phase diagram[13]. In addition, there are studies of p-wave triplet pairing, caused by effective attractive intra-species interaction, proposed for strongly imbalanced cases in two[14] and in three[15, 16] dimensions. In addition to being cooled and trapped, fermionic atoms and mixtures can now also be loaded onto optical lattices[17, 18] where the interaction and the hopping strengths can be tuned, and effects of their interplay with lattice geometry and dimensionality can be probed.

In this Letter, we consider a two-component mixture of fermionic atoms with imbalanced populations on a two-dimensional square lattice. It is well known that the presence of a lattice can provide interesting strong correlation effects, such as spin density wave (SDW) and charge density wave (CDW) phases for fermions on a square lattice at half-filling. Extensive studies can be found in the literature for the case of balanced, SU(2) symmetric fermions, such as the Hubbard model[19] in various lattice geometries and fillings[21–25]. Due to nesting of the Fermi surface (FS), SDW is the dominant instability for the repulsive Hubbard model on a two-dimensional square lattice at half-filling, followed by $d_{x^2-y^2}$-wave superconductivity when the system is doped away from half-filling[23, 24]. When nesting is completely destroyed by doping, the system becomes a normal Fermi liquid, aside from Kohn-Luttinger instabilities[26] at extremely low temperatures. However, when the spin populations are unequal and $SU(2)$ symmetry is broken, both the SDW and the singlet pairing will eventually be precluded due to the mismatch of the FS for the up and down spin fermions at strong population imbalance. From the $SU(2)$ symmetry argument above, singlet pairing will be allowed and dominant in attractive cases when the filling of both species are still close to each other. As the Fermi surfaces become increasingly mismatched, the system is expected to be dominated by other instabilities or becomes a two species Fermi liquid. If the inter-species interaction is initially repulsive, one expects to find SDW phase near the balanced case, switching to other and potentially richer correlated behavior as the polarization increases. Here we study this behavior using a weak-coupling functional renormalization group (fRG) method[22, 24], and obtain the phase diagram for this system, focusing on the case where the majority species stays close to half-filling and the density of the minority species is varied. The phase diagram contains several new phases, including a CDW phase and triplet pairing phases for both species. From our fRG study, we also obtain estimates for the critical energy scales for the different instabilities.

For a microscopic interaction which is on-site, there is no bare intra-species interaction due to Pauli exclusion principle, but an effective long-range interaction can be induced via scattering between species. Previous studies[14–16] have considered such mediated interactions for mixtures of fermion gases (no lattice) with imbalanced populations, finding an attractive effective intra-species pairing interaction, leading to p-wave pairing of the majority species. In this study, we consider the effects of the interplay of interaction, population imbalance, and lattice effects. We show that lattice effects in particular,

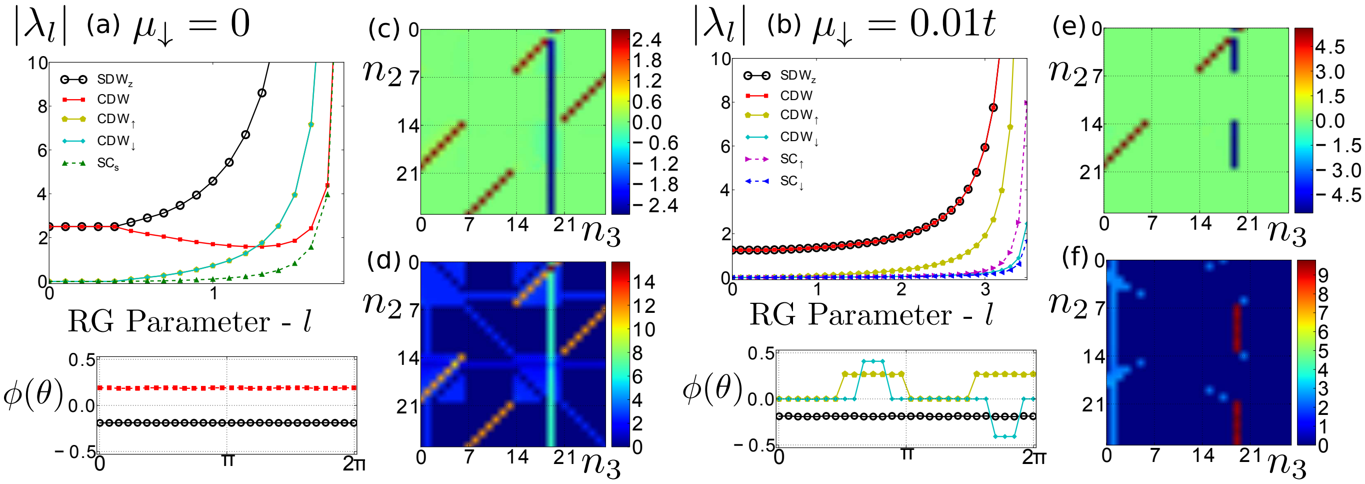

FIG. 1: (a) RG flows of leading eigenvalues of different channels when system is balanced at half-filling, $\mu_\uparrow = \mu_\downarrow = 0$, and the corresponding eigenvectors (M=28). (b) RG flows for density stripe phase at $\mu_\uparrow = 0$, $\mu_\downarrow = 0.01t$. The snapshot of (c) intraspecies vertices $U_{\uparrow\uparrow}(n_1 = 1, n_2, n_3)$ and (d) interspecies $U_{\uparrow\downarrow}(n_1 = 1, n_2, n_3)$ of $\mu_\uparrow = \mu_\downarrow = 0$ near its critical scale. (e) Intraspecies and (f) interspecies are the same plot for $\mu_\uparrow = 0$, $\mu_\downarrow = 0.01t$. The patch indices $n_i = 0 \sim 27$ are show in Fig. 2(i).

not only lead to a much richer phase diagram than that of a imbalanced mixture of fermionic gases, but also with a much higher transition temperature, even at weak interaction couplings, therefore more easily accessible to experimental observation.

1. The model and the fRG method. We consider the one-band Hubbard model for each species ($\sigma = \uparrow, \downarrow$) of fermion (with creation operator $c^\dagger_{\mathbf{k}\sigma}$) on a two-dimensional square lattice, and with on-site s-wave inter-species interaction U_0. The Hamiltonian can be written as:

$$\mathcal{H} = \sum_{\sigma\mathbf{k}} \xi_{\sigma\mathbf{k}} c^\dagger_{\mathbf{k}\sigma} c_{\mathbf{k}\sigma} + \frac{U_0}{V} \sum_{\mathbf{k}\mathbf{k}'\mathbf{q}} c^\dagger_{\mathbf{k}+\mathbf{q}\uparrow} c^\dagger_{\mathbf{k}'-\mathbf{q}\downarrow} c_{\mathbf{k}'\downarrow} c_{\mathbf{k}\uparrow} \qquad (1)$$

, where $\xi_{\sigma\mathbf{k}} = -2t_\sigma(\cos k_x + \cos k_y) + \mu_\sigma$ and V is the volume of the system (hereafter set to be equal to 1). The different chemical potentials μ_σ determine the densities and the hopping amplitude t_σ can be tuned by the optical lattices. In this Letter, we only consider the case $t_\uparrow = t_\downarrow = t$, and weak repulsive inter-species interaction ($U_0 > 0$). There is previous study[20] that shows results of attractive interaction. We neglect the confinement potential for the first approximation.

The fRG approach has been applied to the study of the stability and instabilities of Fermi liquids[22] and has been applied to a number of different lattice models[23–25]. Starting with a microscopic model, the RG method provides an effective theory for low energy scales by integrating out high energy degrees of freedom, reducing the UV cut-off Λ. We perform a zero-temperature one-loop renormalization calculation for the interaction vertices $U_{\sigma\sigma'}(\mathbf{k}_1, \mathbf{k}_2, \mathbf{k}_3, \mathbf{k}_4)$, where $\mathbf{k}_1$ and $\mathbf{k}_2$($\mathbf{k}_3$ and $\mathbf{k}_4$) are the momenta of the incoming(outgoing) fermions, and $\mathbf{k}_1 + \mathbf{k}_2 = \mathbf{k}_3 + \mathbf{k}_4$, shown in Fig.2(a). Figs.2(b)-(f) show the Feynman diagrams that contribute to the renormalized four-leg vertices at one-loop. In order to solve the RG equations, we discretize both FS ($\sigma = \uparrow, \downarrow$) into M patches and integrate the renormalization group equations numerically. We set the cut-off to be $\Lambda_l = 6te^{-l}$, $dl = 0.1$ for an RG step, $U_0 = 2.5t$ and $M = 28$ in all calculations shown here. The bare interaction has no dynamics initially and we neglect self-energy corrections as justified for the one-loop limit[22, 24]. After obtaining RG flows of all marginal interaction vertices that involve states near the Fermi surfaces, we extract vertex combinations that define specific instability channels at each RG step. The pairing channels are $V_{BCS_{\uparrow(\downarrow)}}(\mathbf{k}, \mathbf{q}) = U_{\uparrow\uparrow(\downarrow\downarrow)}(\mathbf{k}, -\mathbf{k}, \mathbf{q}, -\mathbf{q})$, and:

$$\begin{aligned} V_{BCS_{s,t_0}}(\mathbf{k}, \mathbf{q}) \;=\; & \frac{1}{4}(U_{\uparrow\downarrow}(\mathbf{k}, -\mathbf{k}, \mathbf{q}, -\mathbf{q}) \pm U_{\downarrow\uparrow}(\mathbf{k}, -\mathbf{k}, \mathbf{q}, -\mathbf{q}) \\ & + U_{\uparrow\downarrow}(-\mathbf{k}, \mathbf{k}, \mathbf{q}, -\mathbf{q}) \pm U_{\downarrow\uparrow}(-\mathbf{k}, \mathbf{k}, \mathbf{q}, -\mathbf{q})) \end{aligned}$$

where the upper(lower) sign stands for singlet(triplet) pairing. Density wave channels from nesting interactions are given by:

$$\begin{aligned} & V_{SDW_z,CDW}(\mathbf{k}, \mathbf{q}) = \\ & \frac{1}{2}(U_{\uparrow\uparrow}(\mathbf{k}, \mathbf{q}, \mathbf{k}+\mathbf{Q}, \mathbf{q}+\mathbf{Q}) + \mathbf{U}_{\downarrow\downarrow}(\mathbf{k}, \mathbf{q}, \mathbf{k}+\mathbf{Q}, \mathbf{q}+\mathbf{Q}) \\ & \mp U_{\uparrow\downarrow}(\mathbf{k}, \mathbf{q}, \mathbf{k}+\mathbf{Q}, \mathbf{q}+\mathbf{Q}) \mp \mathbf{U}_{\downarrow\uparrow}(\mathbf{k}, \mathbf{q}, \mathbf{k}+\mathbf{Q}, \mathbf{q}+\mathbf{Q})), \end{aligned}$$

where the upper(lower) sign stands for SDW$_z$(CDW) channel, and $\mathbf{Q} = (\pm\pi, \pm\pi)$ is a nesting vector. The pseudo-spin index σ refers to two different hyperfine states of the atoms, thus the term SDW is understood as ordering of the pseudo-spin, and not of real spin. Also, the cold atoms are neutral particles and CDW refers to the number density (not electric charge), but we keep the CDW terminology in analogy to electronic systems. At each RG step, we diagonalize these $M \times M$ matrices as $\sum V_a(\mathbf{k}, \mathbf{q})\phi_a^{(n)}(\mathbf{q}) = \lambda_a^{(n)}\phi_a^{(n)}(\mathbf{k})$. As the leading eigenvalue of a defined channel diverge, we identify it as an instability of the system (the BCS pairing instability requires a negative eigenvalue). The form of the corresponding eigenvector determines the symmetry of the order parameter of the instability.

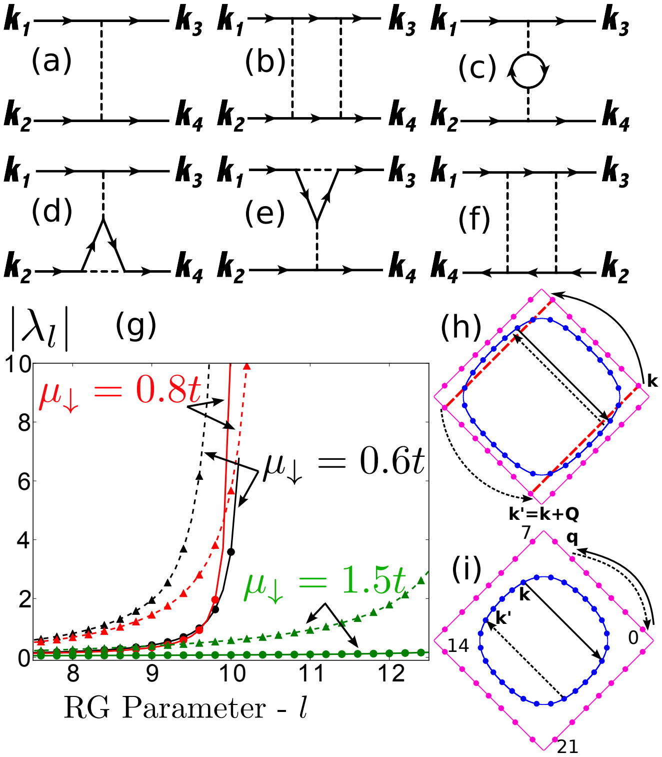

FIG. 2: (a) Definition of interaction vertex. (b)-(f) The one-loop RG corrections to interaction vertices. (g) The RG flow (maker skipped) for majority pairing $BCS_\uparrow$(solid line) and minority pairing $BCS_\downarrow$(dash line) at differnt chemical potential when majority is exactly half-filled, $\mu_\uparrow = 0$. The FS for different filling are shown in (h) $\mu_\downarrow = 0.8t$ and (i) $\mu_\downarrow = 1.5t$, also the patch indices $n = 0 \sim 27$.

2. Nearly balanced case. In order to maximize lattice effects, we focus on the case where the majority species is at or close to half-filling, $\mu_\uparrow \sim 0$, and we vary $\mu_\downarrow$. When the system is balanced ($\mu_\uparrow = \mu_\downarrow = 0$), SDW is the dominant instability (RG flows shown in Fig.1(a)). With increasing $\mu_\downarrow$ the SDW$_z$ order persists for the nearly balanced region (Fig.3). Fig.1(c) and (d) show intensity plots for $U_{\uparrow\uparrow}(k_1, k_2, k_3)$ and $U_{\uparrow\downarrow}(k_1, k_2, k_3)$, at a given RG step, as k_2 and k_3 are varied, covering all patches around the FS (patch index n from 0 to 27), with k_1 fixed at patch $n_1 = 1$. There is an enhanced vertical line at $n_3 = 19$ in these two figures since these patches have $k_1 = k_3 + (\pi, \pi)$, that is, they are related by a nesting vector, and enhanced diagonal lines corresponding to nesting between k_2 and k_3 in Fig.1(d).

3. Weak imbalance. As the minority density is further decreased away from half-filling, some inter-species vertices involving nesting vectors, such as *umklapp* processes, are no longer near the FS and are thus suppressed. However, there are still some non-perfect nesting particle-hole processes with net momentum equal to a reciprocal lattice vector, $(2\pi, 0)$ or $(0, 2\pi)$, which are allowed even under imbalance. An example of such a process is for a minority fermion to scatter from $\mathbf{k} \to \mathbf{k} + \mathbf{Q}_1 - \boldsymbol{\delta}$ across two opposite sides of its FS (say along the 45° direction), while a majority fermion scatters from $\mathbf{q} \to \mathbf{q} + \mathbf{Q}_2 + \boldsymbol{\delta}$ across the other two opposite sides of its FS (say along the 135° direction). With $\mathbf{Q}_1 = (\pi, \pi)$, $\mathbf{Q}_2 = (-\pi, \pi)$, and $\boldsymbol{\delta} = (\delta, \delta)$ accounting for the FS mismatch, the net momentum for this process is $(0, 2\pi)$ and therefore of *umklapp*-type and allowed by momentum conservation in spite of the imbalance. These vertices can still renormalize significantly under RG flow, and more importantly, they mediate intraspecies nesting processes for the majority fermions, which do have a perfectly nested FS, so these mediated processes have the strongest flow. From a real space picture, with increasing imbalance, both species also have more empty sites to move around to minimize energy and, since the mediated interactions are attractive, this leads to a crossover in the RG flows from the SDW$_z$ to a CDW phase. Fig.1(b) shows the RG flow close to this crossover, where SDW$_z$ and CDW channels are almost degenerate. The lower panel of Fig.1(b) shows the corresponding order parameter symmetries. The CDW channel of both species is doubly degenerate. For one of them, shown in Fig.1(b), the order parameters for ↑ and ↓ are non-zero on two-opposite sides of the FS (second and fourth quadrants), and zero on the other sides (first and third quadrants), with the situation reversed for the other degenerate channel. These correspond to stripe charge order in the diagonal direction. Figs.1(e) and 1(f) show snapshots of the interspecies and majority intraspecies vertices as the instability is approached. Comparing with the $SU(2)$ symmetric case (Fig.1(c) and 1(d)), where the interspecies nesting interaction is the dominant one, when the imbalance is increased ($\mu_\downarrow = 0.01t$), the inter and intraspecies nesting vertices are comparable and carry different signs, indicating that this CDW stripe phase originates from weaker spin fluctuations caused by imbalance in addition to screened intrapecies attraction. Since it involves both spin and charge fluctuations, the size of this region and its critical energy scale depend on the filling fraction of both species (see Fig.3).

4. Strong imbalance. As the imbalance becomes stronger, the FS mismatch precludes all nesting processes as well as zero-momentum singlet pairing. Since the induced intraspecies interactions are always attractive, the dominant RG flows present another crossover, from CDW stripe phase to triplet p-wave BCS pairing. The triplet pairing is for a single fermion species but it is generated by the initial bare interspecies interaction, the lattice (FS shape), and the imbalance (FS mismatch). Whether the dominant pairing is for the majority or for the minority species depends on the interplay of these factors. Fig. 2 shows RG flows for three different minority chemical potentials. As $\mu_\downarrow$ increases, the minority pairing channel is dominant at first. This is because the nearly half-filled majority FS provides a large phase space in RG process to mediate and renormalize the minority intraspecies BCS vertex. The Feynman diagram in Fig. 2(c), which contains an internal fermion loop, gives a first nonzero correction to the intrapecies vertex from two interspecies vertices, of the form,

$$\partial_l U^{(l)}_{\sigma\sigma'}(\mathbf{k}_1, \mathbf{k}_2, \mathbf{k}_3) = \left[1 - \frac{1}{2}(1+X)\delta_{\sigma\sigma'}\right]\beta_{ph}\{U_1, U_2\}, \quad (2)$$

where X denotes the operation $XF(1,2,3,4) = F(2,1,3,4)$ and $\beta_{ph}\{U_1, U_2\} = \Pi\{U_1, U_2\} + \mathcal{T}\Pi\{U_1, U_2\}$, with $\mathcal{T}$ the time-reversal operator and

$$\Pi\{U_1,U_2\}=\sum_{\mathbf{q},\alpha}B_{ph}(\mathbf{k}_1,\mathbf{k}_3,\mathbf{q})U_{\sigma\alpha}(\mathbf{k}_1,\mathbf{q},\mathbf{k}_3)U_{\sigma'\alpha}(\mathbf{k}_4,\mathbf{q},\mathbf{k}_2) \quad (3)$$

where B_{ph} is an integral over an angular sector [24]. From Eq. (3), the induced intraspecies pairing interactions come from integrating out two interspecies interactions. Because the FS of the majority species is flat, there will be more renormalization corrections to intraspecies interaction between minority species at first. For example, in Fig. 2(i), the momentum $\mathbf{q}$ at fixed magnitude can be translated anywhere along that branch of the FS. Fig. 3 shows that the Λ_c for minority pairing decreases monotonically with increasing polarization, because the phase space of induced minority intraspecies pairing becomes smaller. This makes the majority pairing become the dominant instability. The induced pairing interaction of majority species couples to its own nesting channel ($\mathbf{k}$ and $\mathbf{k}'$, for example, are connected by a nesting vector in Fig. 2(h)). Although the initial mediated majority intraspecies pairing interaction is smaller than that for minority species, as discussed above, the strong RG flow through a nesting channel leads to a majority pairing instability. We note that this majority superfluid is not the same as proposed in previous studies of fermion gases[14–16], but is instead a lattice effect and has a much larger energy scale and critical temperature. As the density of minority species is further decreased, it starts to behave like a fermion gas, with a small, almost circular FS, as shown for example in Fig. 2(i). When the density of minority species becomes less than quarter filled, majority pairing vertices involving fermions on opposite sides of the nested FS can no longer be mediated by minority fermions near the minority FS since this momentum would not be conserved. Since the majority species is still perfectly nested, as discussed before, there is more phase space for the minority pairing interactions to be mediated and renormalized. For large minority chemical potential, the critical temperature is much smaller, and eventually reaches our numerical limit ($\Lambda_l \sim 10^{-5}t$). Before this limit is reached, the flow of minority pairing is stronger than majority pairing and other channels. Although we do not obtain a divergence in the minority pairing channel, the system is expected to have a Kohn-Luttinger instability of minority pairing in a rather low critical temperature based on the phase space argument above.

5. Conclusion. We have performed a fRG study of a population imbalanced fermion system on a square optical lattice in two dimensions. When the majority species is close to half-filing, both density wave and triplet pairing phases are highly favorable due to the nesting of majority species FS. At the weak imbalance region, the competition between spin fluctuations and intraspecies attractions leads to a stripe density wave phase, rather than the usual SDW phase. As the imbalance is further increased, p-wave superfluid phases become dominant due to the mismatch of the FS. The competition between majority and minority pairing is determined by their FS geometry and the mediated intraspecies pairing interaction coming from the initial bare interspecies on-site interaction. Both the stripe density wave phase and triplet superfluid phases are enhanced by nesting of the majority FS, leading to much higher critical temperatures than that found for the imbalanced Fermi gas case. According to our calculation, the critical temperature of stripe density wave is roughly $\Lambda_c^{CDW}(\mu_\uparrow=0,\mu_\downarrow=0.01t)\approx 0.18t$ and that of p-wave superfluid is $\Lambda_c^{BCS_\downarrow}(\mu_\uparrow=0.0003t,\mu_\downarrow=0.03t)\approx 0.016t$, where hopping amplitude t can be controlled experimentally.

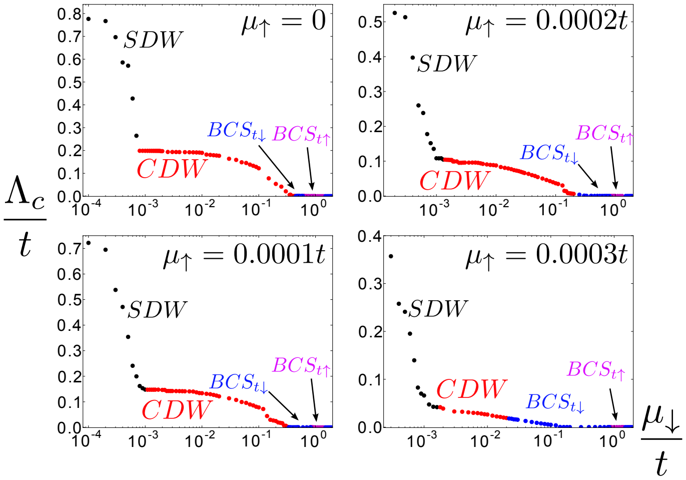

FIG. 3: The estimated critical temperature, $\Lambda_c = 6te^{-l_c}$, of each dominate phase of repulsive model at different majority fillings.

Acknowledgments - We thank Pochung Chen for the computational resources in National Tsing Hua University, Taiwan. SWT thanks Tun Wang for useful discussions in the early stages of this work. We gratefully acknowledge support from NSF under Grant DMR-0847801 and from the UC-Lab FRP under Award number 09-LR-05-118602.

---

[*] Electronic address: shanwent@ucr.edu

[1] M. W. Zwierlein *et al.*, Science **311**, 492 (2006).
[2] G. Partridge *et al.*, Science **311**, 503 (2006).
[3] M. W. Zwierlein *et al.*, Nature (London) **442**, 54 (2006).
[4] Y. Shin *et al.*, Phys. Rev. Lett. **97**, 030401 (2006).
[5] G. Partridge *et al.*, Phys. Rev. Lett. **97**, 190407 (2006).
[6] Y. Shin *et al.*, Nature **451**, 689 (2008).
[7] S. Uji *et al.*, Nature **410**, 908 (2001); *ibidem.*, Phys. Rev. Lett. **97**, 157001 (2006).
[8] W. A. Coniglio *et al.*, Phys. Rev. B **83**, 224507 (2011).
[9] R. Casalbuoni and G. Nardulli, Rev. Mod. Phys. **76**, 263 (2004).
[10] P. Fulde and R. Ferrel, Phys. Rev. **135** A550(1964); A. I. Larkin and Yu. N. Ovchinnikov, Sov. Phys. - *JETP* **20** 762 (1965).
[11] G. Sarma, J. Phys. Chem. Solids **24**, 1092 (1963).
[12] W. V. Liu and F. Wilczek, Phys. Rev. Lett. **90**, 047002 (2003). M. M. Forbes et al., Phys.Rev.Lett. **94**, 017001 (2005). S-T. Wu and S. Yip, Phys. Rev. A **67**, 053603 (2003)
[13] L. Radzihovsky, D. Sheehy, Rep. Prog. Phys. **73**, 076501 (2010).
[14] S. Raghu, and S. Kivelson, Phys. Rev. B **83**, 094518(2011).
[15] A. Bulgac, M. Forbes, and A. Schwenk, Phys. Rev. Lett. **97**, 020402 (2006);
[16] Kelly R. Patton and D. E. Sheehy, Phys. Rev. A **83** 051607

(2011).
[17] J. K. Chin *et al.*, Nature (London) 443, 961 (2006).
[18] T. Stöferle *et al.*, Phys. Rev. Lett. **96**, 030401 (2006)
[19] J. Hubbard, Proc. R. Soc. A **276**, 238 (1963).
[20] M. Inskin and C.A.R. Sá de Melo, Phys. Rev. Lett. **99**, 080403 (2007), and Phys. Rev. A **78**, 013607 (2008).
[21] H. J. Schulz, Europhys. Lett. **4**, 609 (1987).
[22] R. Shankar, Rev. Mod. Phys. **66**, 129 (1994).
[23] C. J. Halboth and W. Metzner, Phys. Rev. B **61**, 7364 (2000).
[24] D. Zanchi and H. J. Schulz, Phys. Rev. B **54**, 9509; Europhys. Lett. **44**, 235(1997); Phys. Rev. B **61**, 13609 (2000).
[25] S.-W. Tsai and J. B. Marston, Can. J. Phys. **79**, 1463 (2001); C. Honerkamp, Phys. Rev. B **68**, 104510 (2003).
[26] W. Kohn and J.M. Luttinger, Phys.Rev.Lett. **15**, 524 (1965).